WINDBLOWN SAND ON MARS: THE EFFECT OF SALTATION THRESHOLD ON DRIFT POTENTIALS DERIVED FROM MARS GCM;

P. Xu, R. Greeley and S. Williams, Dept. of Geology, Arizona State University, Tempe, AZ 85287-1404, J. B. Pollack, Space Science Division, NASA Ames Research Center, Moffett Field, California

INTRODUCTION. The rate at which the wind can redistribute sedimentary material is an important part of any planet's sedimentologic cycle, particularly for Mars, where the competing effects of other gradational processes are less than on Earth. The aeolian drift potential (DP) is a measure of the amount of material capable of being moved through a unit length by the wind for a given period of time [1]. DP is a useful measure of the potential redistribution rate of windblown material on regional scales. The martian aeolian DP was calculated from laboratory studies of sand movement conducted at Martian atmospheric densities and from surface stress, temperature, and pressure values for that region as determined from the Mars General (Atmospheric) Circulation Model (GCM) developed at the NASA/Ames Research Center [2,3]. In our simulations for Mars, DP changes in both magnitude (as expected) and direction if the saltation threshold is altered.

METHOD. The Ames GCM divides the surface of Mars into 7.5° by 9° bins, each with predicted values of pressure, temperature, and surface shear stress. The surface shear vector was used in the saltation flux equation of White [3] to derive DP magnitude and direction for each bin. Seven different values for threshold were used to assess its effect on magnitude and direction of the resultant sand drift. The variation in sand drift direction in a given GCM bin as a function of saltation threshold was analyzed as was the correlation between the calculated sand drift direction and the orientation of aeolian surface features, such as wind streaks.

RESULTS. Threshold shear stresses must be exceeded for a given GCM bin for sand drift to occur. Many bins have no motion, and there is an inverse relationship between the threshold stress and the number of bins reporting sand drift (Figure 1), as well as maximum drift potential value for any given azimuth (Figure 2). Resultant drift directions also change with increasing saltation threshold. The biggest change in direction averaged ~13.25°, which occurs when the threshold increases from 0.008 to 0.016 N/m^2 (Figure 3). The smallest change averaged ~3.6° for an increase in threshold stress from 0.040 to 0.048 N/m^2 (Figure 4). The inverse relationship between saltation threshold and shift in sand drift resultant azimuth reflects the greater variability of gentle winds compared to strong winds.

There is no correlation between the axial orientation of dark (erosional) wind streaks on Mars and the resultant sand drift directions determined in this study (Figure 5). The correlation is much better when bright (depositional) streaks are considered (Figure 6): the best correlation is for a threshold stress of 0.032 N/m^2. The likely explanation for the poor correlation in the case of the dark streaks is that their formation is dominated by local topographic and meteorological conditions that are unaffected by the regional scale parameters utilized by the GCM [5]. Bright streaks form in the aftermath of dust storms when the atmosphere is very stable and less responsive to local conditions [6], hence, bright streak orientation correlate better with the regional sand drift.

CONCLUSIONS. The number of bins which have drift potentials and the maximum drift potential on the planet at one compass direction over the whole year period decrease with increasing threshold. The resultant drift directions also change with increasing threshold. The larger the threshold, the less change in resultant drift direction. The best correlation of bright streaks with resultant drift directions is at a threshold of 0.032 N/m^2.

REFERENCES. [1] Fryberger, S.G. (1979) *U.S.G S. Prof. Paper 1052*, 137-169. [2] Pollack, J.B. et al. (1981) *J. Atmos. Sci. 38*, 3-29. [3] Pollack, J.B. et al. (1990) *JGR. 95*, 1447-1473. [4] White, B.R. (1979) *JGR, 84*, 4643-4651. [5] Greeley, et al. (1993) *JGR, 98*, 3183-3196. [6] Veverka, et al. (1981) *ICARUS, 45*, 154-166.

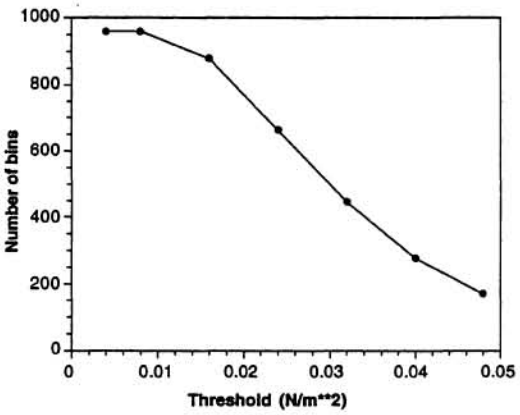

Figure 1. The number of GCM bins which have drift potentials vs. threshold

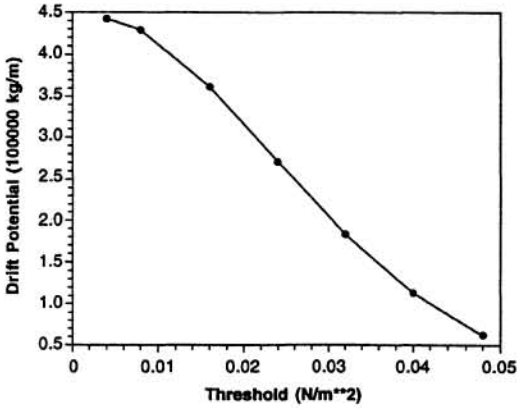

Figure 2. The maximum drift potential on the planet at one compass direction over whole year period vs. threshold

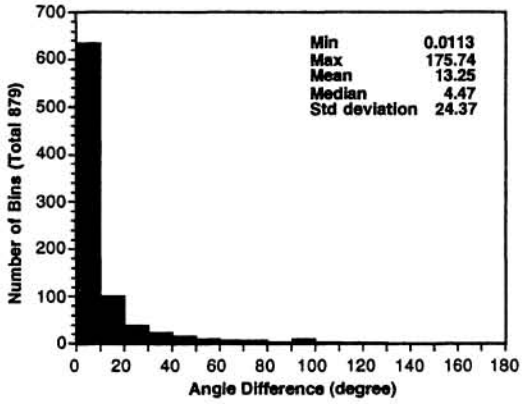

Figure 3. Histogram of angle differences of resultant drift directions from two threshold 0.008 and 0.016 N/m**2

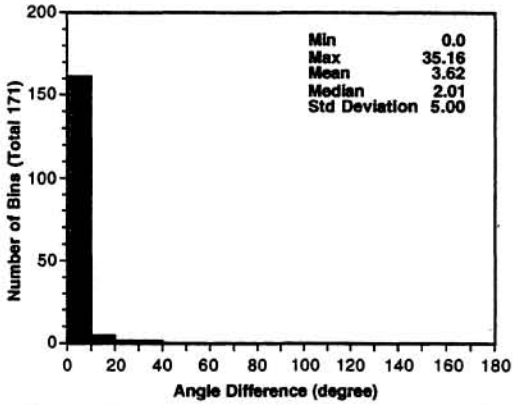

Figure 4. Histogram of angle differences of resultant drift directions from two thresholds 0.040 and 0.048 N/m**2

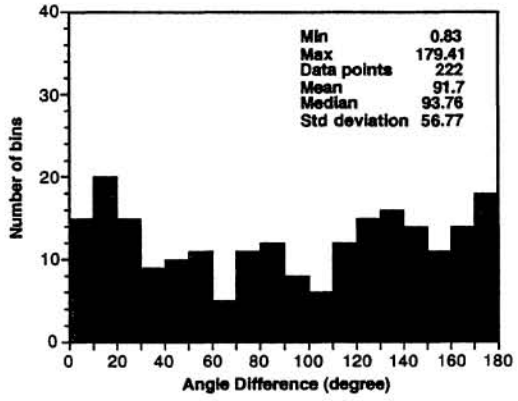

Figure 5. Histogram of angle differences of dark streaks and resultant drift directions at threshold 0.016 N/m**2

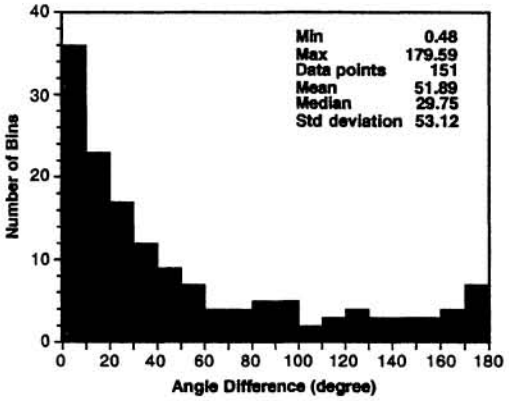

Figure 6. Histogram of angle differences of bright streaks and resultant drift directions at threshold 0.032 N/m**2